Correlation between metal oxidation state and catalytic activity: hydrogenation of crotonaldehyde over Rh catalysts

P. Ferreira-Aparicio [a], B. Bachiller-Baeza [a], I. Rodríguez-Ramos [a], A. Guerrero-Ruiz [b] and M. Fernández-García [a]

[a] *Instituto de Catálisis y Petroleoquímica, CSIC, Campus Cantoblanco, 28049 Madrid, Spain*
[b] *Departamento de Química Inorgánica, UNED, Senda del Rey, 28040 Madrid, Spain*

Received 26 August 1997; accepted 17 October 1997

The effects of the rhodium (oxidation) state on the activity and selectivity for the crotonaldehyde hydrogenation reaction over Rh/Al_2O_3 and Rh/SiO_2 catalysts were examined using the techniques of temperature-programmed reduction, hydrogen chemisorption and X-ray absorption near-edge structure (XANES). In the alumina-supported system, the active phase–support interaction is shown to affect the chemical behavior of rhodium under the influence of a reductive atmosphere by stabilizing Rh^{3+} species. This behavior is not observed (as expected) for Rh/SiO_2 catalysts. The structural and electronic bases of the active phase–support interaction and the effect of the latter phenomenon on the hydrogenation of crotonaldehyde are discussed.

Keywords: rhodium, rhodium–alumina, active phase–support interaction, hydrogenation of crotonaldehyde, temperature-programmed reduction, XANES

1. Introduction

Selective hydrogenation of functional groups in unsaturated compounds has captured the attention of numerous research groups due to its industrial and academic implications [1–6]. Catalysts used in this type of reaction contain a group VIII hydrogenation component (Pt, Rh, . . .) modified and/or in close contact with a second component which main purpose is to increase the probability of a correct adsorption geometry of the unsaturated compound, thereby yielding the desired selectively hydrogenated product. Common second components are cationic base metals (Sn, Mn) [1–3] or metals like Fe that may form alloys with a small ionic contribution to the intermetallic bond and generate surface ''polar'' centers [3–5]. Also, supports that modify the behavior of the group VIII metals are used in obtaining the adequate product [6–8]. Here, we will explore this last option aiming to improving the understanding of the nature of the active phase–support interaction and its influence in the hydrogenation of crotonaldehyde using a Rh/Al_2O_3 system as a catalyst. In addition, a Rh/SiO_2 specimen is included in the study to calibrate the chemical response of Rh in absence of significant support effects. Various studies of the Rh–alumina catalyst have been reported [9–13] but no definitive conclusion regarding the mechanism of the active phase–support interaction has been reached. As (Rh,Al)-mixed oxides are not known [10], the covering of Rh by the alumina support [10], the formation of a non-stoichiometric rhodium oxide phase with oxygen ions shared with alumina [9,11], rhodium oxide raft-like particles [12] or the diffusion of Rh ions into the alumina lattice [10,13], have been claimed to be in the physical ground of the interaction mechanism between rhodium and alumina.

The present paper reports results on the Rh/Al_2O_3 and Rh/SiO_2 catalysts using chemisorption, temperature-programmed reaction (TPR), X-ray absorption near-edge structure (XANES) and the test reaction of crotonaldehyde hydrogenation. The catalytic reaction has been used as a highly sensitive chemical probe to characterize surface species. Our main aim is to establish a correlation between the noble metal (structural and electronic) properties in a system with a strong interaction with the support and its catalytic behavior in the mentioned reaction.

2. Experimental

Catalysts were prepared by impregnation of silica (Aerosil 200, Degussa, 200 m^2/g) or γ-alumina (Puralox Condea, 175 m^2/g) with aqueous solutions of the $RhCl_3$ salt. After calcination at 500°C, composition of the catalysts was determined by atomic absorption spectrometry yielding values of 1.25 and 1.20% for the alumina- and silica-supported systems, respectively. Hydrogen chemisorption measurements were performed in a Micromeritics 2700 Probe Chemisorb apparatus. Samples of 0.4 g were reduced at 400°C (20 cm^3/min hydrogen) during 2 h, cleaned under a flow of Ar and cooled to room temperature, where chemisorption gave values of H/Rh of 0.38 and 0.59 for the Rh/Al_2O_3 and Rh/SiO_2 systems, respectively.

TPR experiments were performed on aliquots of catalysts (0.3 g) placed between two quartz wool plugs in a

U-shaped quartz reactor. A UHP mixture of 6% H_2 in He was fed into the reactor during a temperature ramp of 5°C/min from room temperature to 600°C. Effluents were monitored with a thermal conductivity detector connected to the exit of a Porapack Q column. Individual analyses were performed at intervals of 2.5 min.

XANES experiments at the K-edge were carried out in the ID-24 line at the ESRF Synchrotron, Grenoble. All samples, catalysts and pure reference compounds (i.e. Rh_2O_3, $Rh(CO)_4Cl_2$ and Rh foil), were measured in an energy-dispersive, transmission mode with simultaneous calibration of the energy scale with the help of a Rh foil. A bent perfect Si crystal in a Bragg configuration was used as a dispersive monochromator. Self-supporting wafers of the samples were placed in a controlled-atmosphere (10% H_2 in He) cell and submitted to a heat treatment of 3°C min^{-1} from room temperature to 500°C. Typically, a XANES spectrum was obtained every 10–15°C in a few seconds recording process. The set of XANES spectra taken during the reduction treatment is analyzed using principal component factor analysis (PCA) [14–16]. The PCA analysis assumes that the absorbance in a set of spectra can be mathematically modeled as a linear sum of individual components, called factors, plus noise [15]. To determine the number of individual components, an F-test of the variance associated with factor k and the summed variance associated with the pool of noise factors is performed. A factor is accepted as a pure species (factor associated with signal and not noise) when the percentage of significance level of the F-test, %SL, is lower than a test level recommended by previous experience (5%) [14,16]. The ratio between reduced eigenvalues, R(r), and an empirical function, IND, defined by Malinowsky [15] will be also used in reaching this decision. Once the number of pure components is fixed, XANES spectra corresponding to pure rhodium species and their concentration profiles are generated by a varimax rotation followed by iterative transformation factor analysis [14,16]. XANES-based simulations of the hydrogen consumption produced by rhodium were obtained by deriving the oxidized species (Rh^{3+}) concentration profiles throughout the reduction coordinate.

The hydrogenation of crotonaldehyde was studied in a glass flow microreactor at atmospheric pressure in the temperature range 40–100°C. Catalysts (0.1 g) were previously treated in flowing air at 500°C for 3 h and cooled down to reaction temperature. A mixture of helium, hydrogen and crotaldehyde (98%+, Fluka) with a total flow of 50 ml/min was introduced in the reactor by bubbling the H_2/He gas through a thermostated saturator (277 K) containing the unsaturated aldehyde. Pre-reduction of the catalysts at 100, 200 and 300°C in hydrogen (20 ml/min, 90 min) was also carried out before reaction. The reactor effluents were analyzed by gas chromatography in a Varian 3400 GC using a FID detector and a Cromosorb Carbowax 20M packed column. Crotonaldehyde (CROTAL), crotyl alcohol (CROTOL), butanol (BUTOL), butanal (BUTAL) and butane (BUNE) were the products detected.

3. Results and discussion

The factorial analysis reported in table 1 shows for both catalysts %SL and R(r) values above the cutoff of 5% and approaching one, respectively, from factor 3 upwards. This fact, together with the minimum of the IND function, concurs in pointing out the number of pure species present during the reduction treatment of each catalyst as 2. A detailed picture of the reduction can be extracted from the concentration profiles along the reduction coordinate and, particularly, from the XANES-based simulation of the hydrogen consumption (see figures 1 and 2). While the Rh/SiO_2 specimen presents a well defined temperature of reduction, $\sim$ 100°C, characteristic of big, bulk-like particles of Rh_2O_3 [9], the Rh/Al_2O_3 catalyst is reduced progressively in a broad temperature range (approximately from 30 to 350°C) and shows maxima at about 130 and 185°C. Note that although two maxima are found in the TPR of the last sample, only one oxidized rhodium species is detected by the statistical analysis of the XANES data. This clearly shows that Rh^{3+} has always the same local environment and very similar electronic properties. The corresponding XANES spectra of the Rh^{3+} species evidence in both samples (figure 1b) a distorted octahedral geometry typical of a Rh_2O_3-like phase. The dissimilar thermal behavior of these rhodium catalysts under hydrogen suggests that, in the alumina-supported specimen, the Rh^{3+} ions

Table 1
Principal components factor analysis results

Factor	Eigenvalue	%SL	R(r)	IND×10^4	Variance [a]
		1.25%Rh/Al_2O_3			
1	336.973	0.00	530.37	2.313	99.826
2	0.57401	0.00	127.43	0.422	0.170
3	0.00405	17.42	1.49	0.441	0.001
4	0.00241	23.76	1.13	0.487	0.001
5	0.00188	24.09	0.98	0.545	0.001
6	0.00122	29.40	1.35	0.644	
7	0.00107	26.79	1.02	0.764	
8	0.00066	33.07	1.35	0.986	
		1.20%Rh/SiO_2			
1	266.952	0.00	194.41	6.423	99.546
2	1.21294	0.00	484.32	0.553	0.452
3	0.00218	15.59	1.07	0.581	0.001
4	0.00175	7.63	3.59	0.582	0.001
5	0.00041	28.43	1.37	0.657	
6	0.00024	35.92	0.95	0.919	
7	0.00020	34.72	1.11	1.383	
8	0.00013	37.92	1.31	2.524	

[a] Variance is given as a percentage. Values lower than 10^{-3} are not reported.

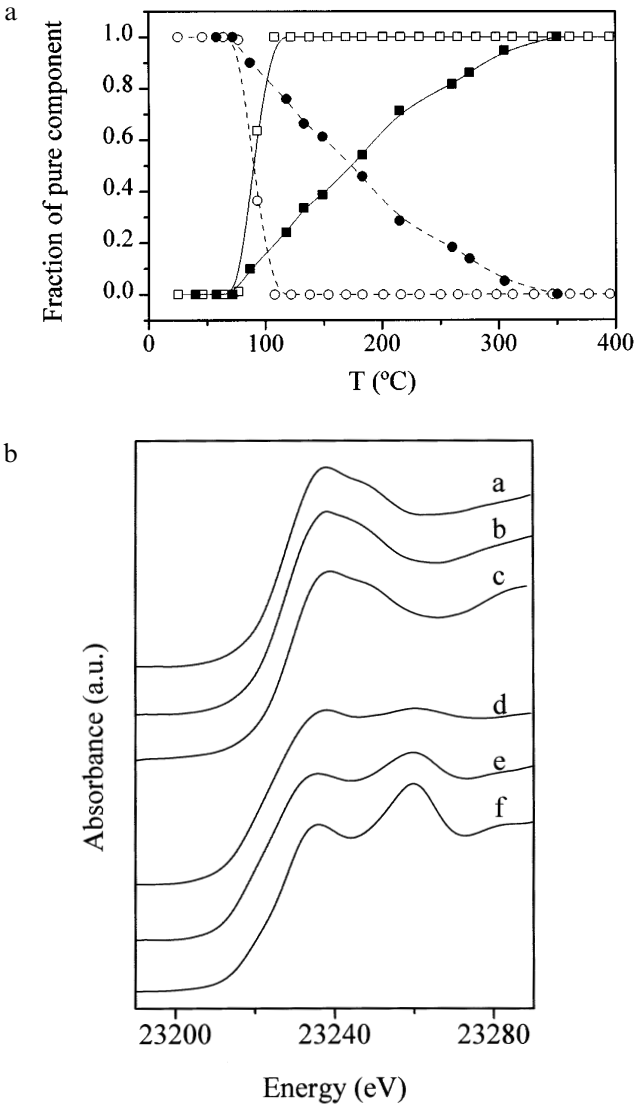

Figure 1. (a) Concentration profiles of the pure rhodium species along the reduction coordinate for Rh/Al_2O_3 (closed symbols) and Rh/SiO_2 (open symbols) catalysts: circles, Rh^{3+} species; squares, Rh^0 species. (b) Predicted pure rhodium species XANES spectra for Rh/Al_2O_3 (a, d) and Rh/SiO_2 (b, e) catalysts. Rh_2O_3 (c) and Rh foil (f) reference XANES spectra are included for comparison.

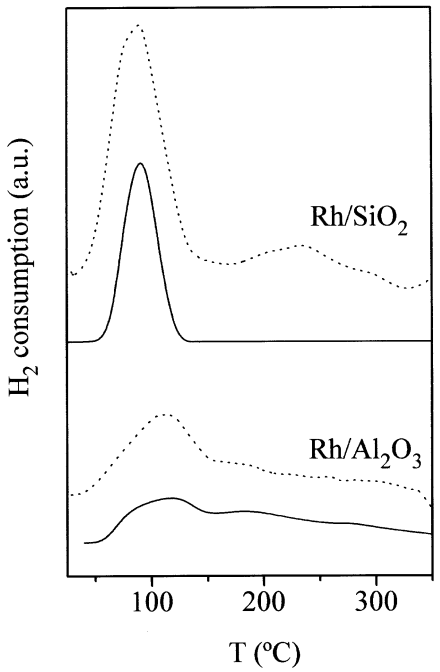

Figure 2. XANES-TPR simulation (full lines) and hydrogen consumption (dashed lines) of the Rh/Al_2O_3 and Rh/SiO_2 systems.

share with superficial Al^{3+} cations some O^{2-} ions of their coordination spheres. The broad temperature range of reduction would then be explained by the different situations for completion of the rhodium coordination sphere with oxygen anions shared or not with alumina; this would induce a finite range of Rh^{3+}–O^{2-} bond stabilities against reduction which, in this case, seems to have two geometrical situations (responsible for the two TPR maxima) with larger probabilities. Notice that this physical picture should not be confused with that corresponding to Rh^{n+} ions inserted in an alumina matrix, which must have a characteristic reduction temperature. Note also that specific (raft-like) particle geometries by itself or the covering by alumina of the active phase do not account for the behavior of the Rh/Al_2O_3 catalyst during TPR experiments; a series of geometrically equivalent Rh^{3+} species with different chemical characteristics of the Rh^{3+}–O^{2-} bond must be postulated in order to interpret the XANES/TPR data. Finally, because the $RhCl_3$ precursor was used to introduce rhodium in the oxide surfaces, Cl^- anions could be present in the rhodium coordination sphere of alumina-supported catalysts [17]; however, the Rh^{3+}–Cl^- coordination distance is close to 2.30 Å, around 0.25 Å larger than the Rh^{3+}–O^{2-} one [18], a fact that should be clearly observed in the XANES spectra. The absence of a significative amount of chlorine was confirmed using XPS and chemical analysis.

The reduction of the oxidic rhodium phases advances in both systems studied without intermediates, e.g. Rh^+ (figure 1). The presence of Rh^{2+} and/or Rh^+ has been reported in several reduced oxide-supported rhodium samples [19] but these partially reduced rhodium species have been usually assigned to isolated cations inserted in oxide vacants, a species of which relative concentration is limited by the factorial XANES analysis to below the detection limit (less than 5% of the total). Rh^+ intermediates should have been manifested in the XANES spectra by their characteristic off-site 4f resonances [20]; the Rh^+ reference complex measured presents them at $\sim$ 23237.5 and 23254.4 eV. The zero-valent phase yielded by the treatment, metallic rhodium, also evidences the strong interaction with the alumina support (figure 1b); the $\sim$ 23235 and 23260 eV continuum resonances appearing at 3 and 1 eV, respectively, shifted to

higher energies with respect to a Rh foil and the Rh/SiO_2 system. These shifts contain chemical (i.e. electronic) and geometrical (i.e. shortening of the Rh–Rh distance) contributions not easily uncoupled. In any event, the less defined continuum resonances and their shifts with respect to a Rh reference system with a similar loading point out that the Rh particles supported by alumina have a noticeably smaller size and are chemically and geometrically influenced by the support; the chemical effects being particularly evident in the 5p sub-band (final state of the 23235 eV continuum resonance [21]). Interesting to stress is the fact that although the Rh/Al_2O_3 catalyst has smaller particles, a smaller H/Rh ratio is obtained, evidencing again the notable chemical implications of the active phase–support interaction. Smaller H/Rh ratios have been consistently reported in alumina-supported systems with respect to silica ones and attributed to the different energy (e.g. chemistry) of the atomic hydrogen –rhodium interaction [22].

The test reaction, hydrogenation of crotonaldehyde, allows to extract some useful conclusions about the stability in both systems. For these two catalysts, catalytic activity and selectivity are summarized in table 2. Catalytic activities are reported within an estimated error of 10%. The first striking difference appears in the activity of both systems; while it grows with the reduction (T_{red}) and reaction (T_{reac}) temperatures for the Rh/Al_2O_3 specimen, for Rh/SiO_2 it grows only with T_{reac} but at $T_{reac} = 60$, 80°C it decreases with T_{red}. Clearly, the absence of stabilizing interactions with the silica support produces the reduction of the rhodium phase even at 40°C and its sintering during reduction pre-treatments at higher temperatures ($\geqslant$100°C). In contrast, the Rh/Al_2O_3 system presents better stability under the reaction mixture and, although with small activity, a 100% selectivity of CROTOL at $T_{reac} = 40$°C. At higher T_{reac} ($\geqslant$60°C) this system is activated but with a parallel loss of selectivity towards the desired unsaturated alcohol (figure 3), this effect being ascribable to the progressive reduction of the active phase in presence of the reductive mixture and the consequent presence of metallic.

The overall reaction data and the physical characterization discussed before allow the conclusion that Rh^{3+} is an active and highly selective species for the selective hydrogenation of CROTAL and that the active phase–support interaction enlarges the lifetime of this species after contact with hydrogen. These results are in line of a recent report, where oxidic $Sn^{\delta+}$ species appear as very selective sites for the hydrogenation of CROTAL to CROTOL [2]. So, the apparent first requisite to get a good selectivity is an oxidic environment which may induce a specific unsaturated compound adsorption geometry. In the case of rhodium, figure 1b suggests that the spreading of rhodium over alumina does not essentially modify the electronic structure of Rh^{3+} cations with respect to bulk-like Rh_2O_3 ones, pointing to a weak or null electronic effect in the reaction. This last point should, however, be taken with caution because reduced rhodium species may be involved in the selective hydrogenation in spite of our failure to detect them in reductive atmospheres. Small amounts of Rh^+/Rh^0 associated with a predominant Rh^{3+} state could be envisaged as the active phase of the reaction. Also, the fact that several oxides (rhodium, tin, ...) are 100% selective in the functional group selective hydrogenation strongly suggests that a geometrical effect cannot play a role in determin-

Table 2
Catalytic properties of the catalysts for the hydrogenation of crotonaldehyde

Catalyst	Pretreatment conditions	Reaction temperature (°C)	Conversion (%)	Activity (μmol/g_{cat} s)	Selectivity (%)			
					CROTOL	BUTAL	BUTOL	BUNE
Rh/Al_2O_3	air 400°C	40	0.2	0.008	100	0	0	0
		60	0.3 [a]	0.011 [a]	100–20	20–100	0	0
		80	1.3	0.060	3	95	0	2
	air 400°C + H_2 100°C	40	2.4	0.112	4	94	2	0
		60	4.0	0.190	0	99	0	1
		80	8.3	0.381	0	98	0	2
	air 400°C + H_2 200°C	40	2.9	0.130	2	95	3	0
		60	6.3	0.287	0	99	0	1
		80	14.2	0.652	0	97	1	2
Rh/SiO_2	air 400°C	40	9.3	0.430	0	99	1	0
		60	21.4	1.039	0	99	0	1
		80	35.3	1.667	0	98	0	2
	air 400°C + H_2 100°C	40	15.7	0.760	0	100	0	0
		60	18.5	0.882	0	100	0	0
		80	30.9	1.554	0	100	0	0
	air 400°C + H_2 200°C	40	13.7	0.750	0	100	0	0
		60	16.0	0.860	0	100	0	0
		80	27.3	1.401	0	99	0	1

[a] Average values. The reaction rate grows with time.

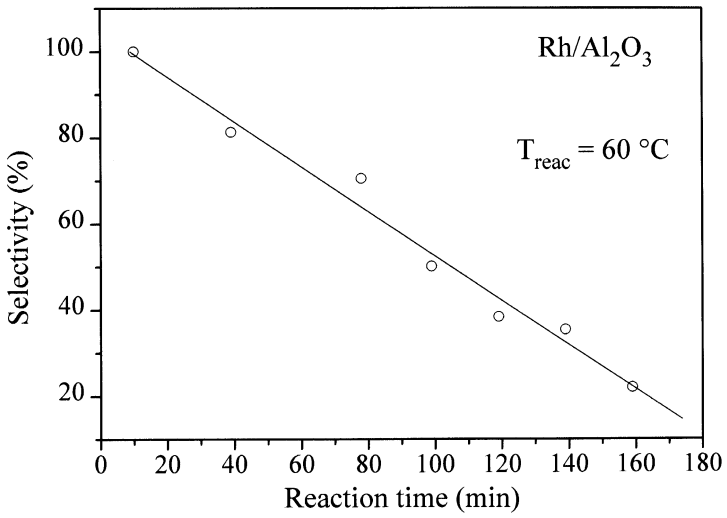

Figure 3. Selectivity (%) to crotyl alcohol versus time on stream for the calcined Rh/Al_2O_3 catalyst at $T_{reac} = 60°C$. A solid line is included to highlight the linear correlation between both parameters.

ing catalytic selectivity. This is in open contrast with pre-reduced Pt or Ru systems, where the structure-sensitivity of the reaction has been observed and theoretically supported (see ref. [6] and references therein).

On the other hand, metallic rhodium is an efficient hydrogen dissociative element that can produce a high concentration of atomic hydrogen in its surface but does not induce the correct geometry of CROTAL adsorption for its selective hydrogenation [1,2]. In our study (gas phase reaction), metallic rhodium shows a high selectivity towards the C=C hydrogenation product, BUTAL, while in liquid phase the hydrogenation proceeds further and the majority product is the saturated alcohol, BUTOL [1].

Acknowledgement

The scientific staff of line ID-24 at the ESRF Synchrotron, Grenoble, is gratefully acknowledged for their help during XANES experiments. MFG thanks the Consejo Superior de Investigaciones Científicas (CSIC) for a postdoctoral contract. This work was supported by DGICYT (Spain) under project number PB94-0077-CO2.

References

[1] P. Gallezot, A. Giroir-Frendler and D. Richart, in: *Catalysis of Organic Reactions*, ed. W. Pascoe (Dekker, New York, 1991).
[2] S. Nishiyama, T. Kubota, K. Kimura, S.Tsuruya and M. Masai J. Mol. Catal. A 120 (1997) L17.
[3] M. English, V.S. Ranade and J.A. Lercher, J. Mol. Catal. A 121 (1997) 69.
[4] T.B.L.W. Marinelli, V. Ponec, C.G. Raab and J.A. Lercher, in: *Heterogeneous Catalysis and Fine Chemicals III*, Stud. Surf. Sci. Catal., Vol. 78 (1993).
[5] V. Ponec and G.C. Bond, *Catalysis by Metals and Alloys* (Elsevier, Amsterdam, 1995).
[6] M. English, A. Jentys and J.A. Lercher, J. Catal. 166 (1997) 25.
[7] M.A. Vannice and B. Sen, J. Catal. 115 (1989) 65.
[8] Z. Poltarzewski, S. Galvano, R. Pietropaolo and P. Staiti, J. Catal. 102 (1986) 190.
[9] R. Burch, P.K. Loader and N.A. Cruise, Appl. Catal. A 147 (1996) 375.
[10] J.G. Chen, M.L. Colaianni, P.J. Chem, J.T. Yates Jr. and G.B. Fischer, J. Phys. Chem. 94 (1990) 5059.
[11] D.D. Beck, T.W. Capehart, C. Wong and D.N. Belton, J. Catal. 144 (1993) 311.
[12] D.J.C. Yates and E.B. Prestridge, J. Catal. 106 (1987) 549.
[13] D.D. Beck and C.J. Carr, J. Catal. 144 (1993) 296.
[14] M. Fernández-García, C. Márquez-Alvarez and G.L. Haller, J. Phys. Chem. 99 (1995) 12565.
[15] E.R. Malinowsky, *Factor Analysis in Chemistry* (Wiley, New York, 1991).
[16] C. Márquez-Alvarez, I. Rodríguez-Ramos, A. Guerrero-Ruiz, G.L. Haller and M. Fernández-García, J. Am. Chem. Soc. 119 (1997) 2905.
[17] K. Lu and B.J. Tatarchuk, J. Catal. 106 (1987) 166.
[18] R.W. Wyckhof, *Crystal Structures* (Wiley, New York, 1963).
[19] A. Martínez-Arias, J. Soria and J.C. Conesa, J. Catal. 168 (1997) 364.
[20] Y. Wu and D.E. Ellis, J. Phys. Condens. Matter 7 (1995) 3973.
[21] T.K. Sham, Phys. Rev. B 31 (1985) 1888.
[22] G.M. Nuñez, A.R. Patrignani and A.J. Rouco, J. Catal. 98 (1986) 554.